

Cite this: *Polym. Chem.*, 2026, **17**, 679

# Molecular insight into a disulfonimide-bearing diol: synthesis, characterisation and access to poly(disulfonimide)s

Denis A. Sapegin, \*<sup>a</sup> Danila A. Kuznetsov,<sup>a</sup> Edward J. Penny, <sup>a</sup>  
Jeremy K. Cockcroft <sup>b</sup> and Joseph C. Bear \*<sup>a</sup>

Control over interchain interactions plays a pivotal role in the design of high-performance polymeric materials. Aromatic polyimides exemplify this principle but still suffer from several inherent limitations in applications requiring high permeability and processability due to dense chain packing. To broaden the design space for advanced polymer architectures, we explore non-planar benzene-1,2-disulfonimide as a promising structural alternative to the conventional imide fragment. This work aims to establish a synthetic and theoretical foundation for the exploration of poly(1,2-disulfonimides) as promising candidates for next-generation high-performance polymers. Here, we perform a comprehensive investigation of the synthetic route to aromatic *N*-substituted cyclic 1,2-disulfonimides and polymers on this basis. The vibrational and geometric features of the disulfonimide fragment were elucidated through a combination of quantum-mechanical calculations and spectroscopic methods, confirming its distinctive structural identity. A synthetic platform for disulfonimide-bearing diols was designed and applied to obtain the first dihydroxy-terminated cyclic 1,2-disulfonimide, which underwent successful model polycondensation. Molecular-dynamics simulations qualitatively indicate that incorporation of the disulfonimide fragment into a polyester backbone leads to a pronounced increase in glass-transition temperature without a corresponding increase in packing density compared to a homologous polyimide.

Received 9th December 2025,  
Accepted 10th January 2026

DOI: 10.1039/d5py01171j

rsc.li/polymers

## Introduction

The synthetic design of specialty polymers is a key research area in materials science, particularly for high-performance and functionally demanding applications. Among polymers being developed for such applications, aromatic polyimides stand out for their exceptional thermal, mechanical, chemical, transport and dielectric performances,<sup>1,2</sup> which arise from strong interchain interactions driven by the electronic structure of the imide fragment and its position in the polymer backbone. Strong interchain interactions are driven by the formation of charge-transfer complexes. The planar electron-deficient imide ring interacts with electron-rich aromatic units along the rigid polymer chain, leading to dense chain packing, a tendency toward amorphous morphology, and elevated glass transition temperatures.<sup>3</sup> While these features contribute to the key properties for which polyimides

are valued, they have several drawbacks that reduce their suitability particularly for applications requiring high permeability and processability.

Since interchain interactions play a major role in determining polyimide properties, their tuning is a key strategy for tailoring performance. However, as long as the imide fragment remains unchanged, the extent of such modification is limited. Broadening the design space therefore requires structural alteration of the fragment itself. In this context, the benzene-1,2-disulfonimide (DSI) fragment offers a structurally related but functionally distinct alternative – featuring non-planar geometry and greater electron deficiency than conventional imides,<sup>4</sup> making it a compelling subject for exploring structure–property relationships in polymer systems. While the non-planarity is expected to prevent packing densification, the enhanced charge separation may compensate by promoting stronger interactions between chains through increased electrostatic cohesion. The presence of four sulfonyl oxygen atoms in each DSI fragment, oriented out-of-plane, provides extensive opportunities for hydrogen bonding and introduces additional interaction sites. Despite their conceptual relevance to polymer design, to the best of our knowledge no synthetic route to

<sup>a</sup>Department of Chemical and Pharmaceutical Sciences, Kingston University, Penrhyn road, Kingston-upon-Thames KT1 2EE, UK.

E-mail: d.sapegin@kingston.ac.uk, j.bear@kingston.ac.uk

<sup>b</sup>Christopher Ingold Laboratories, University College London, London, UK.

Tel: +44 (0) 2076 791004



poly(1,2-disulfonimide)s has been described, and it remains virtually unexplored. We believe that the absence of reported examples may be caused, at least in part, by the synthetic challenges associated with incorporating the DSI fragment into a polymer backbone. It is worth noting, however, that polymers incorporating non-cyclic disulfonimide fragments as side chains – primarily to serve as acidic sites for catalysis or proton conduction – have recently been described.<sup>5,6</sup>

A typical route to DSI ring formation in aromatic systems involves the reaction of substituted 1,2-dichlorosulfonylbenzenes with amines, accompanied by the elimination of HCl.<sup>4,7–9</sup> Unlike the case of conventional imides, this ring-formation reaction is not well-suited for chain extension in polycondensation, as it generally proceeds in modest yields. Given these limitations, a more practical approach to constructing poly(1,2-disulfonimide)s is to preassemble the DSI unit within a bifunctional monomer and then incorporate it into the polymer backbone using well established step-growth polymerisation strategies.<sup>10</sup> The feasibility of this approach depends on the chemical stability of the DSI moiety under the conditions required for the selected functional group transformations and polymerisation.

In this work, we explore a synthetic route to DSI-bearing monomers as novel building blocks for the preparation of poly(1,2-disulfonimide)s *via* polycondensation. Incorporation of the DSI functionality into the polymer backbone offers a means to tailor interchain polarity, with potential implications for chain packing, processability, and transport-related properties. We present a detailed synthetic strategy supported by theoretical and model studies, structural characterization of key intermediates, along with practical considerations for accessing this emerging class of polymers. The viability of the approach is demonstrated through a proof-of-concept polycondensation yielding the first oligomeric species featuring a 1,2-disulfonimide fragment directly integrated into the backbone of a growing chain. Furthermore, the influence of DSI incorporation on polymer properties is assessed by means of molecular dynamics simulations.

## Results and discussion

### Synthesis of the 3,4-bis(chlorosulfonyl)benzoic acid (DCISBA)

The synthesis of the DSI moiety ultimately relies on access to suitably substituted 1,2-dichlorosulfonylbenzene (DCISB) precursors. Most reported strategies involve diazotisation and subsequent substitution of anthranilic<sup>7,8</sup> or *ortho*-amino benzenesulfonic<sup>9</sup> acids. In the benzenesulfonic acid-based approach, diazotisation is followed by substitution of diazonium with sulfur dioxide to give 1,2-disulfonic acid derivatives, which then may be converted to sulfonyl chlorides under relatively harsh conditions (Scheme 1a). However, in the presence of electron-withdrawing substituents, undesired nucleophilic aromatic substitution can occur, making it difficult or impossible to obtain certain DCISBs *via* this method.<sup>4</sup> An alternative route, starting from anthranilic acid derivatives, proceeds through diazotisation followed by decomposition to an aryne intermediate with elimination of CO<sub>2</sub> and N<sub>2</sub>. Trapping with CS<sub>2</sub> in the presence of an alcohol affords a cyclic dithiol intermediate,<sup>11</sup> which can then be oxidized to the corresponding DCISB (Scheme 1b). In contrast to the sulfonic acid route, the dithiol-based approach is more tolerant of substituents and enables access to a broader range of functionalized DCISBs.

From a practical standpoint, 2-aminoterephthalic acid (2-ATA) serves as a highly suitable starting material. It is commercially available, structurally related to anthranilic acid, and bears a carboxylic acid group that provides a convenient handle for the introduction of polycondensation-ready functionality. A one-pot diazotisation–elimination–addition sequence, applied to 2-ATA, affords a carboxylic acid-functionalized benzodithiol, namely 2-(3-methylbutoxy)-2*H*-1,3-benzodithiole-5-carboxylic acid (BDTCA), in high yields (up to 90.8%) following a modified literature procedure.<sup>8</sup> The primary byproduct is terephthalic acid, typically formed when the reaction temperature is insufficient to drive the elimination step to completion. A characteristic signal at 7.12 ppm in the <sup>1</sup>H NMR spectrum (in DMSO-d<sub>6</sub>), correlated by HSQC and HMBC experiments to a shift at 90.7 ppm in the <sup>13</sup>C NMR

#### a) 2-amino-benzenesulfonic acid route



#### b) Anthranilic acid route

**Scheme 1** Comparison of 2 approaches to DCISB synthesis: (a) amino-benzenesulfonic acid route; (b) anthranilic acid route.



spectrum, was attributed to the intersulfur carbon. Notably, this  $^{13}\text{C}$  signal appears in a distinct region of the spectrum, unusual for typical aromatic or aliphatic carbons, making it a convenient diagnostic marker for the presence of the cyclic dithiol fragment.

Oxidation of BDTCA with chlorine in the presence of water, or alternatively *via* a more convenient laboratory-scale protocol using  $\text{SOCl}_2$  and  $\text{H}_2\text{O}_2$ ,<sup>12</sup> leads to 3,4-bis(chlorosulfonyl) benzoic acid (DCISBA) in good overall yields (67–77% based on 2-ATA). The full synthetic pathway is outlined in Fig. 1a.

DCISBA features a highly electron-deficient aromatic system due to the presence of three strongly electron-withdrawing substituents. The molecular structure, confirmed by single-crystal X-ray diffraction (SXD) (CCDC 2497755, in SI: Tables S3a–e and Fig. S6–S8), is a layered solvate with *p*-xylene with orthorhombic space-group symmetry *Pbam*. As is common for organic acids, the molecules form dimers due to hydrogen bonding between the  $-\text{CO}_2\text{H}$  groups of adjacent molecules within the crystallographic plane (Fig. 1c).

The crystal structure reveals that the chlorosulfonyl groups in the 3 and 4 positions on the aromatic ring adopt a conformation to avoid steric interaction of the Cl atoms, with one above and the other below the plane of the ring. Given that the Cl atom of the chlorosulfonyl group in the 3-position can be either above or below the plane of the ring, this leads to disorder of this group in both the 3- and 4-position about the mirror plane in the crystal structure. The steric interaction of the adjacent chlorosulfonyl groups is seen in the angle subtended by the two sulfur atoms with the centroid of the aromatic ring, which deviates from the ideal  $60^\circ$  to about  $71.5^\circ$

(Fig. 1b). The observed strain caused by steric hindrance of the bulky chlorosulfonyl groups, which is also likely to occur in *ortho*-benzenedisulfonic acids, together with the electron deficiency of the aromatic core, may explain the tendency of such systems to undergo aromatic substitution, as reported for the reaction of 3,4-disulfobenzoic acid with  $\text{SOCl}_2$ .<sup>4</sup> Carboxylic acid dimerization observed in the SXD (Fig. 1c) was also detected by FTIR spectroscopy (full spectra in SI – Fig. S5), which shows a characteristic  $\text{C}=\text{O}$  stretching band at  $1704\text{ cm}^{-1}$ ,<sup>13</sup> along with bands at  $1388$  and  $1179\text{ cm}^{-1}$  attributed to  $\text{S}=\text{O}$  stretching in the sulfonyl chloride,<sup>14</sup> and a band at  $860\text{ cm}^{-1}$  corresponding to  $\text{C}-\text{H}$  bending in the 1,2,4-substituted benzene core.<sup>15</sup>

### Synthesis of bifunctional 1,2-benzenedisulfonimides

In the same vein as a well-established strategy for the synthesis of poly(amide-imide)s, it was decided to incorporate the DSI moiety into a dicarbonyl chloride, enabling subsequent polycondensation with aromatic amines.<sup>4,10</sup> The approach requires the synthesis of a DSI-diacid followed by its conversion to the corresponding dicarbonyl chloride.

To access a simple aromatic di-carboxy-terminated 1,2-disulfonimide, *p*-aminobenzoic acid (PABA) was chosen as the amine component for the reaction with DCISBA due to its commercial availability and the abundance of literature data on its analogous imide derivatives.<sup>16–19</sup> However, contrary to expectations, the reaction of DCISBA with PABA, as well as with its methyl ester and more nucleophilic aromatic diamines such as 4,4'-oxydianiline and *m*-phenylenediamine, failed to produce the desired 1,2-disulfonimide products. This outcome



Fig. 1 (a) Synthetic route to DCISBA; (b) molecular (c) and dimeric structures of DCISBA as determined by single-crystal X-ray diffraction.



persisted despite extensive variation of reaction parameters, including acid scavengers and catalysts (pyridine, triethylamine,  $\text{Na}_2\text{CO}_3$ ), temperature (room temperature to 130 °C), and solvents (DMSO,  $\text{H}_2\text{O}$ , NMP, DMF, acetonitrile, chloroform). The observed reactivity of the DCISBA substrate is most likely explained by the presence of a free carboxylic acid group. The electron-deficient nature of the DCISBA core increases its acidity, while the basic conditions of the reaction medium, arising from the presence of HCl scavengers, may facilitate partial deprotonation of the corresponding carboxylate. We hypothesise that the nucleophilic attack by this carboxylate on the chlorosulfonyl group of a second DCISBA molecule could lead to the formation of mixed anhydride intermediates, which may subsequently undergo aminolysis to yield amide-containing byproducts.<sup>20</sup>  $^1\text{H}$  NMR spectra of the crude reaction mixtures of DCISBA with 4,4'-oxydianiline and *m*-phenylenediamine show signals in the range of  $\delta = 9.5\text{--}11$  ppm, consistent with amide (NH) protons and supportive of the hypothesised reaction pathway.

To overcome this, we introduced methyl ester protection to both coupling partners in an effort to facilitate formation of the target 1,2-disulfonimide diester. Protection of the carboxylic acid group in BDTCA was achieved *via* Fischer esterification, yielding methyl 2-methoxy-2*H*-1,3-benzodithiole-5-carboxylate (BDTCA-Me) in a moderate yield (37.0% based on BDTCA and 33.1% based on 2-ATA). Notably, during the investigation of the BDTCA esterification products, a new polymorph of dimethyl terephthalate (DMT) was identified by the means of SXD (CCDC 2497754, in SI: Tables S2a–e and Fig. S3–

S4). Previously the crystal structure was reported as orthorhombic (refcode DMTPAL in the Cambridge Crystallographic Database<sup>21</sup>), while this new form is triclinic with two distinct crystallographic molecules within the unit cell.

The nucleophilic substitution at the methylene carbon between the thiol sulfurs of the BDTCA was observed to proceed more rapidly than esterification, as indicated by time-course  $^1\text{H}$  NMR monitoring of the reaction mixture while tracking signals corresponded to the methyl groups of the ether – 3.13 ppm and ester – 3.83 ppm functionalities, as well as the carboxylic acid proton – 13.15 ppm (Fig. S2 and Table S1). This behavior is consistent with earlier findings on the behaviour of such dithiol systems, as reported by Sarhan *et al.* and Nakayama.<sup>11,22</sup> Subsequent oxidation of BDTCA-Me gave methyl 3,4-bis(chlorosulfonyl)benzoate (DCISBA-Me) in good isolated yield for the step (76% which translates to 23.5% for 2-ATA). As expected, the reaction of DCISBA-Me with methyl *p*-aminobenzoate (PABA-Me), in 1,2-dichloroethane at reflux, afforded the target 1,2-disulfonimide diester, 4-[2-methoxycarbonyl]-*N*-(*p*-methoxycarbonylphenyl)benzene-1,2-disulfonimide (DSI-PABA-Me), in a moderate isolated yield of 39.4%. The reaction required harsher conditions than those reported for the formation of the analogous dimethyl DSI derivative,<sup>4</sup> proceeding cleanly only upon reflux in 1,2-dichloroethane (DCE, 82 °C) in the presence of pyridine (Fig. 2a).

The structure of DSI-PABA-Me was thoroughly characterized using a combination of  $^1\text{H}$  and  $^{13}\text{C}$  NMR spectroscopy, including HMBC experiments, as well as FTIR spectroscopy. The FTIR spectrum was interpreted with the aid of density func-



**Fig. 2** (a) Synthesis of DSI-PABA-Me; (b) geometry-optimised structure obtained *via* DFT calculations, highlighting distortion of planarity in the PABA core and non-planarity of the DSI cycle; (c)  $^1\text{H}$ – $^{13}\text{C}$  HMBC spectrum showing key correlations supporting structural assignment; (d) Modelled and experimental FTIR spectra of DSI-PABA-Me confirming characteristic functional group vibrations.



tional theory (DFT) predicted vibrational modes, enabling confident assignment of key bands to characteristic sulfonimide and ester functionalities (Fig. 2d, Fig. S9a–b and Table S4). Bands in the range 572–948  $\text{cm}^{-1}$ , along with ones at 1171  $\text{cm}^{-1}$  and in 1222–1248  $\text{cm}^{-1}$  range, were attributed to deformation modes of the DSI ring. A band at 1112  $\text{cm}^{-1}$  corresponded to  $-\text{SO}_2$  stretching, while the band at 1212  $\text{cm}^{-1}$  was assigned to methyl wagging vibrations of the ester group. The attribution of the characteristic bands of the FTIR spectra agreed well with those reported for other aromatic 1,2-disulfonimides.<sup>4</sup> Notably, in the  $^{13}\text{C}$  NMR spectrum, the carbon atom adjacent to the sulfonimide nitrogen exhibited an upfield shift from 151.6 ppm in PABA-Me to 129.0 ppm in DSI-PABA-Me in  $\text{CDCl}_3$ . This carbon was clearly correlated in the HMBC spectrum with protons on the adjacent aromatic ring (Fig. 2c). The observed increase in shielding of the *ipso* carbon provides strong evidence for electronic density redistribution, likely resulting from reduced conjugation between the nitrogen lone pair and the adjacent PABA-Me core. Evaluation of the lowest-energy conformer of DSI-PABA-Me (Fig. 2b and Table S5), obtained through geometry optimisation using DFT methods, reveals a “twisted” conformation of the PABA core that disrupts planarity and hinders delocalisation of the nitrogen lone pair into the aromatic system, consistent with the observed upfield shift. This structural distortion closely resembles the electronic changes associated with aniline protonation – namely, loss of conjugation and a transition in nitrogen hybridisation towards  $\text{sp}^3$ -like character, accompanied by a characteristic upfield shift of the *ipso* carbon (aniline: 148.1 ppm; anilinium ion: 135.7 ppm).<sup>23</sup> The predicted non-planarity of the DSI core (C–S–N–S–C) further supports this interpretation, consistent with a partially  $\text{sp}^3$ -hybridised nitrogen environment. Collectively, these findings provide strong evidence for successful formation of the 1,2-disulfonimide linkage.

Several deprotection strategies have been applied to obtain corresponding 1,2-disulfonimide-bearing diacid from DSI-PABA-Me,<sup>24,25</sup> including acidic and basic hydrolysis in different conditions, however DSI cycle could not withstand the attempted deprotections as was evidenced by the disappearance of the characteristic 129.0 ppm shift on the  $^{13}\text{C}$  spectra. Sadly, direct attempts at polycondensation of the obtained diester with various aromatic diamines following the procedures described in<sup>26,27</sup> did not produce target poly(1,2-disulfonimide)s.

It was therefore clear that a softer deprotection may be needed, and a reductive cleavage of benzyl esters was considered a suitable strategy. To obtain a corresponding dibenzyl terminated DSI, benzyl 2-(3-methylbutoxy)-2*H*-1,3-benzodithiole-5-carboxylate (BDCTA-Bn) was synthesised from the sodium salt of BDTCA and benzyl chloride following a well-known procedure.<sup>28</sup> As expected due to the different reaction mode (carboxylate anion acting as nucleophile instead of being the substrate) the substitution in the inter-sulfur carbon was not observed and the yields in which BDCTA-Bn was obtained were greater (52.56% for stage and 41.33% for 2-ATA). Oxidation of BDCTA-Bn to a corresponding DCISB followed by

a condensation reaction with benzyl *p*-aminobenzoate in a procedure analogous to that used for the methyl ester, afforded 4-[2-benzyloxycarbonyl]-*N*-(*p*-[2-benzyloxycarbonyl]phenyl)benzene-1,2-disulfonimide (DSI-PABA-Bn) in a yield of 32.94% and allowed to test various reductive deprotections.<sup>29,30</sup> Contrary to our expectations, the DSI cycle was not able to withstand hydrogenation as indicated by the  $^1\text{H}$  NMR and HMBC (the characteristic *ipso* carbon shift at  $\sim 129.0$  ppm disappeared). It became clear that the synthetic route to the target diacid is hindered by the limited stability of the DSI moiety in the deprotection conditions. Other protection routes, involving the synthesis of BDTCA carboxyl chloride were also considered suitable. However, attempts to prepare it by treating BDTCA with various chlorinating agents ( $\text{SOCl}_2$ ,  $\text{POCl}_3$ ) under mild conditions resulted in degradation of the dithiol ring (as was evidenced by the disappearance of the characteristic shifts at 7.12 ppm on  $^1\text{H}$  and 90.7 ppm on  $^{13}\text{C}$  spectra) leaving a mixture of unidentified products behind.

### Modular access to 1,2-disulfonimide diols *via* alkylation with primary-halogenated alcohols

Due to the incompatibility of the DSI cycle with a number of deprotection conditions examined, deprotection-based synthesis of DSI-dicarboxylic-acid proved impractical; however, *O*-alkylation of BDTCA provides access to bifunctional 1,2-disulfonimides, as demonstrated by the examples of DSI-PABA-Me and DSI-PABA-Bn. These results suggested an alternative route to 1,2-disulfonimide-bearing monomers: the introduction of alkyl substituents bearing functional groups suitable for polycondensation, which could remain intact during the DSI cycle formation.

Hydroxyl groups appeared as particularly promising candidates. Widely employed as linkages in the synthesis of polyesters and other step-growth polymers, they offer excellent compatibility with polycondensation strategies. Although hydroxyl groups are known to react with chlorosulfonyls to yield sulfonate esters under basic conditions,<sup>31</sup> the higher reactivity of amines is expected to ensure that DSI-fragment formation predominates. The synthetic focus was therefore shifted from a DSI-diacid-chloride to a DSI-diol. Accordingly,  $\text{S}_\text{N}2$ -type alkylation of BDTCA with alcohols bearing a halogen on a primary carbon is proposed as a straightforward route to a family of DSI diols, thereby establishing a modular platform for subsequent polycondensation (Scheme 2). This approach, however, is inherently limited to aliphatic fragments due to the constraints of carboxylic acid *O*-alkylation<sup>32</sup> and the inaccessibility of the BDTCA-derived acid chloride. As a result, the synthesis of fully aromatic poly(1,2-disulfonimides) remains unattainable *via* this route.

To verify the applicability of the general approach suggested, BDTCA was alkylated with 2-chloroethanol using the procedure described in<sup>33</sup> to obtain crude 2-hydroxyethyl 2-(3-methylbutoxy)-2*H*-1,3-benzodithiole-5-carboxylate (BDTCA-EtOH). The presence of the hydroxyl group promoted substitution at the intersulfur carbon, resulting in a mixture of products bearing various substituents at this position, as evi-





**Scheme 2** General approach for the synthesis of DSI-based diols.

denced by multiple signals around the characteristic shift of 7.12 ppm in the  $^1\text{H}$  NMR spectrum. Nevertheless, the major component corresponded to 2-hydroxyethyl substitution at the carboxylic acid. Since the subsequent oxidative conversion of dithiols to dichlorosulfonyls involves cleavage of the dithiol ring, the presence of a mixed substitution at the intersulfur carbon was not expected to interfere with this transformation. Accordingly, crude BDTCA-EtOH was carried forward to the next stage without purification. Crude BDTCA-EtOH was oxidised following a standard procedure to afford 2-hydroxyethyl 3,4-bis(chlorosulfonyl)benzoate (DCISBA-EtOH) in a moderate yield (20.0% for 2-ATA) and acceptable purity ( $\sim 90\%$ ). The comparable yields of DCISBA-EtOH and DCISBA-Me (23.5% for 2-ATA) suggest that the preceding alkylation step affording BDTCA-EtOH proceeded with an efficiency similar to that observed for BDTCA-Me.

The condensation of DCISBA-EtOH with 2-hydroxyethyl *p*-aminobenzoate (PABA-EtOH), obtained from *p*-aminobenzoic acid *via* alkylation with 2-chloroethanol, was carried out in a 2 : 1 THF/DCE solvent mixture (Fig. 3a). The choice was necessary due to the poor solubility of PABA-EtOH in DCE. The procedure followed was analogous to that used previously for the synthesis of other DSI compounds. The reaction afforded 4-[2-hydroxyethoxycarbonyl]-*N*-(*p*-{4-hydroxyethoxycarbonyl}phenyl) benzene-1,2-disulfonimide (DSI-PABA-EtOH) in a yield of 10.4%. As expected, this was lower than the values observed for other DSIs, likely due to the presence of hydroxyl groups. Nevertheless, the outcome is acceptable for laboratory-scale synthesis and supports the viability of the proposed strategy for DSI formation *via* condensation of hydroxyl-containing DCISBs and amines to afford DSI-diols. Further optimization would be beneficial for scale-up, both in the alkylation steps



**Fig. 3** (a) Synthesis of DSI-PABA-EtOH; (b)  $^1\text{H}$ - $^{13}\text{C}$  HMBC spectrum showing key correlations supporting structural assignment; (c) FTIR spectrum of DSI-PABA-EtOH confirming characteristic functional group vibrations and its comparison with the experimental spectra of DSI-PABA-Me.



and in the subsequent DSI-forming condensation – providing an opportunity for future research in this area. The structure of hydroxyl-terminated DSI-PABA-EtOH was confirmed by a combination of NMR experiments ( $^1\text{H}$ ,  $^{13}\text{C}$ , and HMBC) and FTIR spectroscopy.

As DSI-PABA-EtOH was found to be insoluble in chloroform, NMR spectra were acquired in DMSO- $d_6$ . Due to the change in solvent for the NMR acquisition, some proton signals exhibited noticeable shifts compared to DSI-PABA-Me; however, the overall spectral pattern remained consistent, as expected (Fig. 3b). The presence of a characteristic carbon resonance near 129.0 ppm, which was previously assigned to the carbon adjacent to the disulfonimide nitrogen (Fig. 2c), supports successful DSI ring formation. Free hydroxyl protons were observed in the  $^1\text{H}$  NMR spectrum as triplets at 5.09 ppm (DCISBA core) and 4.97 ppm (PABA core). Corresponding FTIR data further supported these findings, showing a broad bimodal O–H stretching band at 3100–3400  $\text{cm}^{-1}$  and a sharp C–O stretching band at 1075  $\text{cm}^{-1}$ , both of which are absent in the FTIR spectrum of DSI-PABA-Me (Fig. 3c). Additional FTIR bands attributed to characteristic sulfone vibrations and disulfonimide ring modes (Fig. S10 and Table S6) corresponded well with those observed for DSI-PABA-Me, confirming their structural similarity.

During the formation of DSI-PABA-EtOH, an oily precipitate separated from the reaction mixture. Given the known insolubility of pyridinium hydrochloride in ethers such as THF,<sup>34</sup> the precipitate was hypothesized to consist mainly of pyridinium salts. NMR analysis of both the supernatant and precipitated

phases confirmed that the oily phase predominantly contained pyridinium species, while the desired product was present in both phases. To investigate the impact of reaction heterogeneity on yield, several experiments were conducted using alternative solvents. Similar reactions performed in acetonitrile and DMF proceeded homogeneously but afforded significantly lower yields (~3% in acetonitrile; no product isolated from DMF). The reduced yield in acetonitrile was attributed to possible side reactions between the solvent and the chlorosulfonyl group.<sup>35</sup> In the case of DMF, the complete absence of isolated product was unexpected, but it may be explained by the formation of a catalytic complex between DMF and the chlorosulfonyl species,<sup>36</sup> potentially promoting an undesired reaction pathway over DSI formation, for reasons that remain unclear. These results suggest that polar, non-coordinating solvents could be more favourable for DSI formation, though further investigation is needed to support this conclusion.

### Polycondensation and computational assessment of DSI-induced effects on polymer properties

To evaluate the polycondensation capability of DSI-PABA-EtOH, a micro-scale model reaction with terephthaloyl chloride (TPA) was carried out in deuterated THF in the presence of triethylamine at room temperature (Fig. 4a). Prior to the reaction, the DSI diol was dried under vacuum at 40 °C for 48 h. However, the  $^1\text{H}$  NMR spectrum of the purified diol in THF- $d_8$  still revealed traces of water, evidenced by a singlet at  $\delta$  2.46 ppm,<sup>37</sup> underscoring the high hygroscopicity of the monomer. To compensate for residual moisture, TPA was used



Fig. 4 (a) Model polycondensation of DSI-PABA-EtOH with terephthaloyl chloride (TPA) affording poly(DSI-TPA) oligomers. (b)  $^1\text{H}$ - $^{13}\text{C}$  HMBC spectrum showing key cross-peaks confirming diester linkage formation and the incorporation of the DSI moiety.



in excess. The model polycondensation was allowed to proceed for 24 h, after which the reaction mixture was analysed by NMR spectroscopy (Fig. 4b).

Precipitation of triethylamine hydrochloride from the reaction mixture was accompanied by the appearance of new resonances in the  $\delta$  4.70–4.40 ppm region, assigned to the methylene protons of the ethylene fragment in the esterified oligomeric species. These protons exhibited HMBC correlations with the carbonyl carbons of the terephthaloyl fragment ( $\delta$  = 165.0 ppm ester C=O) and those of the PABA and DCISBA cores ( $\delta$  = 164.6 and 163.0 ppm, respectively), confirming the formation of aliphatic ester linkages between the diol and the dichloride components.

The resonance at  $\delta$  8.25 ppm was assigned to aromatic protons of unreacted TPA (added in excess). The multiplet at  $\delta$  8.18–8.05 ppm is most plausibly attributed to mono-adducts of TPA formed with water and/or the diol, as indicated by HMBC correlations to carbons at  $\delta$  ~165 ppm (carboxylic acid/ester C=O) and  $\delta$  161.1 ppm (acyl chloride C=O), which overlap with signals from the PABA aromatic ring (arising from both unreacted and esterified species). The overlapping resonances at  $\delta$  8.03–7.95 ppm can be assigned to terephthaloyl units incorporated into the target di-ester linkages, which is further supported by its correlation to carbons at  $\delta$  165.0 ppm (ester C=O) on the HMBC (Fig. 4b). The signals at  $\delta$  7.66–7.61 ppm are attributed to PABA-ring protons, with overlapping contributions from the monomer and the esterified product. HMBC spectra further showed that the carbon signal adjacent to the DSI nitrogen remained at approximately  $\delta$  129 ppm, indicating that the DSI moiety

remained chemically intact throughout the reaction. Despite employing a fourfold excess of TPA, the  $^1\text{H}$  NMR data suggest a conversion of roughly 50%, most likely limited by residual water in the reaction mixture; the resonances of the esterified monomer appear slightly upfield and partially overlap with those of the unreacted diol.

The NMR results (Fig. 4b) collectively confirmed the formation of poly(4-[2-ethoxycarbonyl]-*N*-(*p*-[4-ethoxycarbonyl]phenyl)benzene-1,2-disulfonimide benzene-1,4-dicarboxylate) (poly(DSI-TPA), Fig. 4a) oligomers, marking the first incorporation of a 1,2-disulfonimide fragment directly into a backbone of a growing chain. While these results demonstrate the inherent reactivity of the DSI-diols toward polycondensation, its hygroscopic character and limited availability hindered the synthesis of high-molecular-weight polymers, primarily due to challenges in drying and purification at this scale. Nevertheless, the proof-of-concept polycondensation reaction demonstrates the viability of the proposed synthetic platform, establishing a foundation for future studies on poly(1,2-disulfonimide)s and the investigation of their structural, morphological, mechanical, thermophysical, and other key properties.

To obtain qualitative molecular-level insight into how the DSI fragment may affect key polymer characteristics such as glass-transition temperature and chain packing, we performed a series of comparative molecular dynamics simulations on model systems of poly(DSI-TPA), a homologous polyimide (PI-TPA), and parent polyethylene terephthalate (PET) (Fig. 5 and S1). It should be noted that the modelling was performed for the corresponding amorphous phases of all polymers considered.

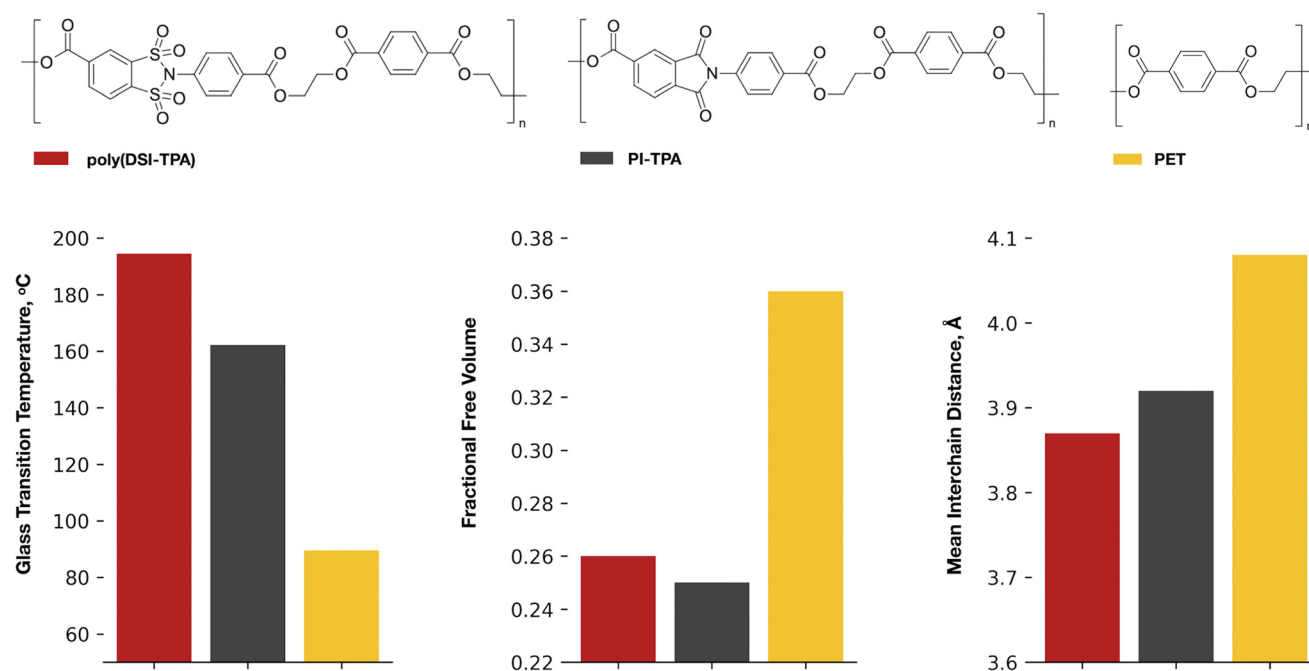


Fig. 5 Comparison of the glass-transition temperature (°C), fractional free volume (290 K), and mean interchain distance (290 K, Å) of amorphous poly(DSI-TPA), PI-TPA and PET samples, obtained from molecular dynamics simulations.



The simulations provided PET with a glass transition temperature ( $T_g$ ) of 89 °C, which is higher than typical experimental values (65–92 °C<sup>38</sup>). The difference is expected, given the very fast cooling rate used in the modelling (4 ns per 10 °C;  $\sim 6 \times 10^9$  °C s<sup>-1</sup>) which leads to overestimation of  $T_g$  values. Still, the result is close enough to experimental data to show that the approach provides a reliable comparative estimate. At 290 K, the fractional free volume (FFV) decreases from 0.361 in PET to 0.262 in poly(DSI-TPA), indicating tighter chain packing, consistent with the reduction in mean interchain distance from 4.08 Å to 3.87 Å. The accompanying increase in density from 1.263 to 1.390 g cm<sup>-3</sup> is consistent with the incorporation of heavy sulfone groups within the disulfonimide unit. Based on analysis of the monomer structures, we expected the DSI-based fragment to produce a larger increase in  $T_g$  through stronger interchain interactions and higher segmental inertia, while its non-planar geometry was anticipated to counteract this effect by limiting packing densification. The simulations support this hypothesis: the polyimide analogue exhibits a lower  $T_g$  of 162 °C but nearly identical packing characteristics (FFV = 0.251; mean interchain distance = 3.92 Å). It should be noted that the present comparison is based on computational models and establishes a compelling basis for further experimental exploration.

## Conclusion

In this study, we present a practical approach to the synthesis of 1,2-disulfonimide-bearing diols as a straightforward pathway towards poly(1,2-disulfonimide)s. The benzodithiol route proved to be a suitable entry point to bifunctional aromatic *N*-substituted benzene 1,2-disulfonimides and their polymeric derivatives. Application of the suggested synthetic approach enabled the preparation and characterisation of a representative series of 1,2-disulfonimide diesters. The instability of the considered heterocycle under ester hydrolysis and reductive deprotection conditions was identified, defining practical limits for further functionalisation. The combination of computational and spectroscopic methods enabled detailed elucidation of the geometrical features of the disulfonimide fragment and allowed precise assignment of the characteristic FTIR bands. The structure of the carboxy-functionalised 1,2-dichlorosulfonylbenzene model precursor, determined by single-crystal X-ray diffraction, revealed a highly strained geometry that helps to explain both the moderate yields and limited stability of the disulfonimide fragment, as well as the characteristic substitution behaviour of the corresponding 1,2-benzenedisulfonic acids under chlorination conditions. A synthetic platform for disulfonimide-containing monomers was established *via* *O*-alkylation of cyclic benzenedithiol carboxylic acids with primary halogenated alcohols. Aromatic amines containing primary hydroxyl groups reacted with corresponding dichlorosulfonylbenzene intermediates to afford target disulfonimides in acceptable yields. The first-in-class diol, synthesised from hydroxyethoxy-esters of *p*-aminobenzoic

and 3,4-bis(chlorosulfonyl)benzoic acids underwent model polycondensation with terephthaloyl chloride to yield oligomers containing the disulfonimide unit within the backbone.

Molecular-dynamics simulations revealed that incorporation of the non-planar, highly polar disulfonimide fragment is projected to markedly increase the glass-transition temperature without increasing packing density, identifying its future potential as a promising structural motif for high-performance polymers that provides a way to enhance thermal stability without compromising chain packing.

## Conflicts of interest

The authors declare no conflict of interest.

## Data availability

The data supporting this article are available in the Supplementary Information (SI): experimental and computational methods, materials, synthetic procedures, characterisation of new compounds, density-temperature plots obtained via molecular dynamics simulations and additional data from computational methods, FTIR, NMR and SXD. See DOI: <https://doi.org/10.1039/d5py01171j>.

The authors have cited additional references within the SI.<sup>39–47</sup> Crystallographic data for DCISBA (CCDC 2497755) and a new polymorph of dimethylterephthalate (CCDC 2497754) have been deposited with the Cambridge Crystallographic Data Centre (CCDC).

CCDC 2497754 and 2497755 contain the supplementary crystallographic data for this paper.<sup>48a,b</sup>

## References

- 1 *Polyimides*, ed. D. Wilson, H. D. Stenzenberger and P. M. Hergenrother, Springer Netherlands, 1990. DOI: [10.1007/978-94-010-9661-4](https://doi.org/10.1007/978-94-010-9661-4).
- 2 H. Ohya, V. V. Kudryavtsev and S. I. Semenova, *Polyimide Membranes: Applications, Fabrications and Properties*, Routledge, London, 1997. DOI: [10.1201/9780203742969](https://doi.org/10.1201/9780203742969).
- 3 M. Fryd, *Polyimides*, 1984, 377–383, DOI: [10.1007/978-1-4615-7637-2\\_25](https://doi.org/10.1007/978-1-4615-7637-2_25).
- 4 D. A. Sapegin, D. A. Kuznetsov and J. C. Bear, Synthesis of aromatic 1,2-disulfonimides and their prospects as monomers, *New J. Chem.*, 2023, **47**, 5270–5279, DOI: [10.1039/D2NJ06005A](https://doi.org/10.1039/D2NJ06005A).
- 5 G. Giorgianni, M. E. Casacchia, F. Pescioli, P. C. Ricci, S. Di Muzio, A. Lazzarini and A. Carlone, New Polymeric Disulfonimide for Heterogeneous Silicon Lewis Acid Catalysis, *Synlett*, 2024, 426–430, DOI: [10.1055/a-2349-1863](https://doi.org/10.1055/a-2349-1863).
- 6 S. C. Sutradhar, S. Yoon, T. Ryu, L. Jin, W. Zhang, W. Kim and H. Jang, Branched Sulfonimide-Based Proton Exchange Polymer Membranes from Poly(Phenylenebenzophenone)s for Fuel Cell Applications,



- Membranes*, 2021, **11**, 168, DOI: [10.3390/membranes11030168](https://doi.org/10.3390/membranes11030168).
- 7 M. Barbero, S. Bazzi, S. Cadamuro, L. Di Bari, S. Dughera, G. Ghigo, D. Padula and S. Tabasso, Synthesis of 3-aryl-4-methyl-1,2-benzenedisulfonimides, new chiral Brønsted acids. A combined experimental and theoretical study, *Tetrahedron*, 2011, **67**, 5789–5797, DOI: [10.1016/j.tet.2011.05.127](https://doi.org/10.1016/j.tet.2011.05.127).
- 8 M. Barbero, S. Berto, S. Cadamuro, P. G. Daniele, S. Dughera and G. Ghigo, Catalytic properties and acidity of 1,2-benzenedisulfonimide and some of its derivatives. An experimental and computational study, *Tetrahedron*, 2013, **69**, 3212–3217, DOI: [10.1016/j.tet.2013.02.053](https://doi.org/10.1016/j.tet.2013.02.053).
- 9 K. Sørbye, C. Tautermann, P. Carlsen and A. Fiksdahl, *N,N*-1,2-Benzenedisulfonylimide, a new cyclic leaving group for the stereoselective nucleophilic substitution of amines, *Tetrahedron: Asymmetry*, 1998, **9**, 681–689, DOI: [10.1016/S0957-4166\(98\)00033-0](https://doi.org/10.1016/S0957-4166(98)00033-0).
- 10 *Synthetic Methods in Step-Growth Polymers*, M. E. Rogers and T. E. Long, 2003. DOI: [10.1002/0471220523](https://doi.org/10.1002/0471220523).
- 11 J. Nakayama, A One-Step Synthesis of 2-Alkoxy-1,3-benzodithioles, *Synthesis*, 1975, 38–39, DOI: [10.1055/s-1975-23654](https://doi.org/10.1055/s-1975-23654).
- 12 K. Bahrami, M. M. Khodaei and M. Soheilzad, Direct Conversion of Thiols to Sulfonyl Chlorides and Sulfonamides, *J. Org. Chem.*, 2009, **74**, 9287–9291, DOI: [10.1021/jo901924m](https://doi.org/10.1021/jo901924m).
- 13 L. J. Bellamy, *The Infrared Spectra of Complex Molecules*, 1980, 128–194. DOI: [10.1007/978-94-011-6520-4\\_5](https://doi.org/10.1007/978-94-011-6520-4_5).
- 14 L. J. Bellamy, *The Infrared Spectra of Complex Molecules*, 1980, pp. 221–239. DOI: [10.1007/978-94-011-6520-4\\_7](https://doi.org/10.1007/978-94-011-6520-4_7).
- 15 D. Lin-Vien, N. B. Colthup, W. G. Fateley and J. G. Grasselli, *The Handbook of Infrared and Raman Characteristic Frequencies of Organic Molecules*, 1991, pp. 277–306. DOI: [10.1016/B978-0-08-057116-4.50023-7](https://doi.org/10.1016/B978-0-08-057116-4.50023-7).
- 16 N. V. Afanas'eva, G. N. Gubanov, K. A. Romashkova, D. A. Sapegin and S. V. Kononova, Relaxation processes in an aromatic polyamide-imide and composites on its basis with hydrosilicate nanoparticles, *Polym. Sci., Ser. A*, 2016, **58**, 956–967, DOI: [10.1134/S0965545X16060018](https://doi.org/10.1134/S0965545X16060018).
- 17 D. A. Sapegin, G. N. Gubanov, E. N. Popova and S. V. Kononova, Increasing the performance of asymmetric pervaporation membranes for the separation of methanol/methyl-*tert*-butyl ether mixtures by the introduction of sulfonated polyimide into the poly(amide-imide) matrix, *J. Appl. Polym. Sci.*, 2021, **138**(10), 49982, DOI: [10.1002/app.49982](https://doi.org/10.1002/app.49982).
- 18 S. V. Kononova, D. A. Sapegin, E. V. Kruchinina, G. N. Gubanov, K. A. Romashkova, A. L. Didenko, V. E. Smirnova, E. N. Popova, N. N. Saprykina, E. N. Vlasova and V. M. Svetlichnyi, Preparation, structure, and pervaporation performance of poly(amide-imide)-sulfonated polyimide composites, *J. Appl. Polym. Sci.*, 2019, **136**(45), 48197, DOI: [10.1002/app.48197](https://doi.org/10.1002/app.48197).
- 19 D. A. Sapegin, G. N. Gubanov, S. V. Kononova, E. V. Kruchinina, N. N. Saprykina, A. Ya. Volkov and M. E. Vylegzhanina, Characterisation of Romakon™-PM pervaporation membranes for the separation of dilute aqueous alcohol mixtures, *Sep. Purif. Technol.*, 2020, **240**, 116605, DOI: [10.1016/j.seppur.2020.116605](https://doi.org/10.1016/j.seppur.2020.116605).
- 20 K. Wakasugi, A. Nakamura, A. Iida, Y. Nishii, N. Nakatani, S. Fukushima and Y. Tanabe, Novel and efficient method for esterification, amidation between carboxylic acids and equimolar amounts of alcohols, and amines utilizing Me<sub>2</sub>NSO<sub>2</sub>Cl and *N,N*-dimethylamines; its application to the synthesis of coumapherine, a natural chemopreventive dieneamide, *Tetrahedron*, 2003, **59**, 5337–5345, DOI: [10.1016/S0040-4020\(03\)00734-8](https://doi.org/10.1016/S0040-4020(03)00734-8).
- 21 F. Brisse and S. Pérez, Etudes conformationnelles de dérivés d'oligométhylène glycols et de composés apparentés. V. Structure cristalline et moléculaire du téréphtalate de méthyle, C<sub>10</sub>H<sub>10</sub>O<sub>4</sub>, *Acta Crystallogr., Sect. B: Struct. Sci.*, 1976, **32**, 2110–2115, DOI: [10.1107/S0567740876007218](https://doi.org/10.1107/S0567740876007218).
- 22 A. E.-W. Sarhan and T. Izumi, An Efficient Synthesis of 2-(3-methylbutoxy)-1,3-benzodithiole, *J. Chem. Res.*, 2002, **2002**, 11–12, DOI: [10.3184/030823402103170475](https://doi.org/10.3184/030823402103170475).
- 23 T. Axenrod, M. J. Wieder, T. Khin, G. A. Webb, H. J. C. Yeh and S. Bulusu, <sup>13</sup>C NMR: Substituent effects on one-bond 15N-13C coupling constants in anilines and anilinium ions, *Org. Magn. Reson.*, 1979, **12**, 1–4, DOI: [10.1002/mrc.1270120102](https://doi.org/10.1002/mrc.1270120102).
- 24 S. Mattsson, M. Dahlström and S. Karlsson, A mild hydrolysis of esters mediated by lithium salts, *Tetrahedron Lett.*, 2007, **48**, 2497–2499, DOI: [10.1016/j.tetlet.2007.02.029](https://doi.org/10.1016/j.tetlet.2007.02.029).
- 25 C. J. Salomon, E. G. Mata and O. A. Mascaretti, Recent developments in chemical deprotection of ester functional groups, *Tetrahedron*, 1993, **49**, 3691–3734, DOI: [10.1016/S0040-4020\(01\)90225-X](https://doi.org/10.1016/S0040-4020(01)90225-X).
- 26 F. Jouffret and P.-J. Madec, Polyamide synthesis by ester aminolysis. I. A new route for nylon-6,6 synthesis, *J. Polym. Sci., Part A: Polym. Chem.*, 1996, **34**, 2363–2370, DOI: [10.1002/\(SICI\)1099-0518\(19960915\)34:12%3C2363::AID-POLA10%3E3.0.CO;2-6](https://doi.org/10.1002/(SICI)1099-0518(19960915)34:12%3C2363::AID-POLA10%3E3.0.CO;2-6).
- 27 N. Ogata, K. Sanui, T. Ohtake and H. Nakamura, Solution Polycondensation of Diesters and Diamines Having Hetero Atom Groups in Polar Solvents, *Polym. J.*, 1979, **11**, 827–833, DOI: [10.1295/polymj.11.827](https://doi.org/10.1295/polymj.11.827).
- 28 S. Sivakumar, V. G. Pangarkar and S. B. Sawant, Homogeneous System for the Synthesis of Benzyl Salicylate, *Org. Process Res. Dev.*, 2002, **6**, 149–151, DOI: [10.1021/op010058d](https://doi.org/10.1021/op010058d).
- 29 P. K. Mandal and J. S. McMurray, Pd-C-Induced Catalytic Transfer Hydrogenation with Triethylsilane, *J. Org. Chem.*, 2007, **72**, 6599–6601, DOI: [10.1021/jo0706123](https://doi.org/10.1021/jo0706123).
- 30 J. Khurana and R. Arora, Rapid Chemoselective Deprotection of Benzyl Esters by Nickel Boride, *Synthesis*, 2009, 1127–1130, DOI: [10.1055/s-0028-1087982](https://doi.org/10.1055/s-0028-1087982).
- 31 B. A. Stenfors and F. N. Ngassa, Sulfonamides and sulfonate esters: Synthetic routes, proposed mechanisms, and crystallographic characterizations, *Eur. J. Chem.*, 2024, **15**, 282–290, DOI: [10.5155/eurjchem.15.3.282-290.2557](https://doi.org/10.5155/eurjchem.15.3.282-290.2557).



- 32 W. P. Weber and G. W. Gokel, *Reactivity and Structure: Concepts in Organic Chemistry*, 1977, 85–95. DOI: [10.1007/978-3-642-46357-0\\_6](https://doi.org/10.1007/978-3-642-46357-0_6).
- 33 H. C. Heim and C. F. Poe, PREPARATION OF SOME GLYCOL BENZOATES, *J. Org. Chem.*, 1944, **09**, 299–301, DOI: [10.1021/jo01186a001](https://doi.org/10.1021/jo01186a001).
- 34 M. D. Taylor and L. R. Grant, Preparation of anhydrous pyridine hydrochloride, *J. Chem. Educ.*, 1955, **32**, 39, DOI: [10.1021/ed032p39](https://doi.org/10.1021/ed032p39).
- 35 Y. Markushyna, M. Antonietti and A. Savateev, Synthesis of Sulfonyl Chlorides from Aryldiazonium Salts Mediated by a Heterogeneous Potassium Poly(heptazine imide) Photocatalyst, *ACS Org. Inorg. Au*, 2021, **2**, 153–158, DOI: [10.1021/acsorginorgau.1c00038](https://doi.org/10.1021/acsorginorgau.1c00038).
- 36 J. D. Albright, E. Benz, A. E. Lanzilotti and L. Goldman, Reactions of sulphonyl chloride–NN-dimethylformamide complexes, *Chem. Commun.*, 1965, 413–414, DOI: [10.1039/C19650000413](https://doi.org/10.1039/C19650000413).
- 37 G. R. Fulmer, A. J. M. Miller, N. H. Sherden, H. E. Gottlieb, A. Nudelman, B. M. Stoltz, J. E. Bercaw and K. I. Goldberg, NMR Chemical Shifts of Trace Impurities: Common Laboratory Solvents, Organics, and Gases in Deuterated Solvents Relevant to the Organometallic Chemist, *Organometallics*, 2010, **29**, 2176–2179, DOI: [10.1021/om100106e](https://doi.org/10.1021/om100106e).
- 38 N. M. Alves, J. F. Mano, E. Balaguer, J. M. Meseguer Dueñas and J. L. Gómez Ribelles, Glass transition and structural relaxation in semi-crystalline poly(ethylene terephthalate): a DSC study, *Polymer*, 2002, **43**, 4111–4122, DOI: [10.1016/S0032-3861\(02\)00236-7](https://doi.org/10.1016/S0032-3861(02)00236-7).
- 39 F. Neese, The ORCA program system, *Wiley Interdiscip. Rev.: Comput. Mol. Sci.*, 2011, **2**, 73–78, DOI: [10.1002/wcms.81](https://doi.org/10.1002/wcms.81).
- 40 T. A. Halgren, Merck molecular force field. I. Basis, form, scope, parameterization, and performance of MMFF94, *J. Comput. Chem.*, 1996, **17**, 490–519, DOI: [10.1002/\(SICI\)1096-987X\(199604\)17:5/6<490::AID-JCC1>3.0.CO;2-P](https://doi.org/10.1002/(SICI)1096-987X(199604)17:5/6<490::AID-JCC1>3.0.CO;2-P).
- 41 P. Eastman, R. Galvelis, R. P. Peláez, C. R. A. Abreu, S. E. Farr, E. Gallicchio, A. Gorenko, M. M. Henry, F. Hu, J. Huang, A. Krämer, J. Michel, J. A. Mitchell, V. S. Pande, J. P. Rodrigues, J. Rodriguez-Guerra, A. C. Simmonett, S. Singh, J. Swails, P. Turner, Y. Wang, I. Zhang, J. D. Chodera, G. De Fabritiis and T. E. Markland, OpenMM 8: Molecular Dynamics Simulation with Machine Learning Potentials, *J. Phys. Chem. B*, 2023, **128**, 109–116, DOI: [10.1021/acs.jpcc.3c06662](https://doi.org/10.1021/acs.jpcc.3c06662).
- 42 W. L. Jorgensen, D. S. Maxwell and J. Tirado-Rives, Development and Testing of the OPLS All-Atom Force Field on Conformational Energetics and Properties of Organic Liquids, *J. Am. Chem. Soc.*, 1996, **118**, 11225–11236, DOI: [10.1021/ja9621760](https://doi.org/10.1021/ja9621760).
- 43 L. S. Dodda, I. Cabeza de Vaca, J. Tirado-Rives and W. L. Jorgensen, LigParGen web server: an automatic OPLS-AA parameter generator for organic ligands, *Nucleic Acids Res.*, 2017, **45**, W331–W336, DOI: [10.1093/nar/gkx312](https://doi.org/10.1093/nar/gkx312).
- 44 S. V. Lyulin, A. A. Gurtovenko, S. V. Larin, V. M. Nazarychev and A. V. Lyulin, Microsecond Atomic-Scale Molecular Dynamics Simulations of Polyimides, *Macromolecules*, 2013, **46**, 6357–6363, DOI: [10.1021/ma401163z](https://doi.org/10.1021/ma401163z).
- 45 S. V. Lyulin, S. V. Larin, A. A. Gurtovenko, V. M. Nazarychev, S. G. Falkovich, V. E. Yudin, V. M. Svetlichnyi, I. V. Gofman and A. V. Lyulin, Thermal properties of bulk polyimides: insights from computer modeling versus experiment, *Soft Matter*, 2014, **10**, 1224, DOI: [10.1039/C3SM52521J](https://doi.org/10.1039/C3SM52521J).
- 46 L. Martínez, R. Andrade, E. G. Birgin and J. M. Martínez, PACKMOL: A package for building initial configurations for molecular dynamics simulations, *J. Comput. Chem.*, 2009, **30**, 2157–2164, DOI: [10.1002/jcc.21224](https://doi.org/10.1002/jcc.21224).
- 47 R. E. H. Kuveke, L. Barwise, Y. van Ingen, K. Vashisth, N. Roberts, S. S. Chitnis, J. L. Dutton, C. D. Martin and R. L. Melen, An International Study Evaluating Elemental Analysis, *ACS Cent. Sci.*, 2022, **8**, 855–863, DOI: [10.1021/acscentsci.2c00325](https://doi.org/10.1021/acscentsci.2c00325).
- 48 (a) CCDC 2497754: Experimental Crystal Structure Determination, 2026, DOI: [10.5517/ccdc.csd.cc2pv3qd](https://doi.org/10.5517/ccdc.csd.cc2pv3qd); (b) CCDC 2497755: Experimental Crystal Structure Determination, 2026, DOI: [10.5517/ccdc.csd.cc2pv3rf](https://doi.org/10.5517/ccdc.csd.cc2pv3rf).

